Enhanced electron correlations at the $Sr_xCa_{1-x}VO_3$ surface

J. Laverock,[1] J. Kuyyalil,[1] B. Chen,[1] R. P. Singh,[2,*] B. Karlin,[3] J. C. Woicik,[3] G. Balakrishnan,[2] and K. E. Smith[1,4]

[1]*Department of Physics, Boston University, 590 Commonwealth Avenue, Boston, Massachusetts 02215, USA*

[2]*Department of Physics, University of Warwick, Coventry CV4 7AL, United Kingdom*

[3]*Materials Science and Engineering Laboratory, National Institute of Standards and Technology, Gaithersburg, Maryland 20899, USA*

[4]*School of Chemical Sciences and MacDiarmid Institute for Advanced Materials and Nanotechnology, University of Auckland, Auckland 1142, New Zealand*

(Received 24 October 2014; revised manuscript received 8 April 2015; published 20 April 2015)

We report hard x-ray photoemission spectroscopy measurements of the electronic structure of the prototypical correlated oxide $Sr_xCa_{1-x}VO_3$. By comparing spectra recorded at different excitation energies, we show that 2.2 keV photoelectrons contain a substantial surface component, whereas 4.2 keV photoelectrons originate essentially from the bulk of the sample. Bulk-sensitive measurements of the O $2p$ valence band are found to be in good agreement with *ab initio* calculations of the electronic structure, with some modest adjustments to the orbital-dependent photoionization cross sections. The evolution of the O $2p$ electronic structure as a function of the Sr content is dominated by A-site hybridization. Near the Fermi level, the correlated V $3d$ Hubbard bands are found to evolve in both binding energy and spectral weight as a function of distance from the vacuum interface, revealing higher correlation at the surface than in the bulk.

DOI: 10.1103/PhysRevB.91.165123 PACS number(s): 71.27.+a, 73.20.−r, 79.60.−i, 71.20.−b

I. INTRODUCTION

The broad family of complex correlated oxides is the next frontier in novel materials, providing a rich variety of tunable properties that are both functionally useful and valuable in understanding fundamental condensed matter physics. For example, interfaces between perovskite-type oxides are relatively easily achieved at an atomically precise scale, yielding new and exciting properties [1]. As these materials become more important, achieving a firm understanding of their surfaces, including the role and degree that electron correlations play, is crucial.

In strongly correlated materials, the on-site Coulomb energy U leads to dynamical correlations between electrons, tending towards their localization at atomic sites. Incoherent electron states, the Hubbard subbands, form either side of the coherent, one-electron-like quasiparticle peak (QP), and are referred to as lower and upper Hubbard bands (LHBs and UHBs, respectively). Transfer of spectral weight away from the QP into the LHB and UHB signals the effects of stronger electron correlations. Such strong correlations can have profound effects on the electronic structure and material properties, most famously leading to insulating, rather than metallic, ground states [2].

$Sr_xCa_{1-x}VO_3$ are prototypical strongly correlated perovskites, with similar spectral weight in both the incoherent (strongly correlated) Hubbard subbands and the coherent (one-electron-like) quasiparticle states. Although the spectral function of these materials has been well studied experimentally [3–12] and theoretically [13–17], there is not a well-established consensus on the form of the surface and bulk components, or as the Sr content (x) is varied. Both end members are correlated metals and have been reported to exhibit metal-insulator transitions in ultrathin films due to a reduction in the dimensionality and corresponding narrowing of the V $3d$ bandwidth [18]. Generally, the focus of photoemission spectroscopy (PES) studies has been on obtaining bulk-representative spectra. For example, laser-PES has been used at very low photon energies, below the minimum in the photoelectron inelastic mean free path (IMFP), to extract bulk QP spectra [6], although the LHB is not accessible at these low energies. Conversely, soft x rays have also been used to increase the depth sensitivity, and PES spectra were obtained which were either independent of x [4] or which revealed an insulating surface [8]. More recently, some progress has been made in understanding the behavior of the spectra with x, with several reports agreeing that the LHB of $CaVO_3$ is more intense and closer to the Fermi level E_F than that of $SrVO_3$ [7,9], indicative of the effects of stronger electron correlations. Additionally, band dispersions and Fermi surfaces have been clearly observed in both end members [5,7,12]. However, the behavior of the spectra at the surface compared with the bulk has received little experimental attention, despite the role of the surface being questioned and studied in detail theoretically [13,15]. Moreover, our knowledge of the "bulk" spectra from PES has so far been limited to analytical differences between spectra containing both bulk and surface components [4,6,8,9].

Recently, resonant soft x-ray emission spectroscopy (RXES) measurements have reported truly bulk-representative information on the strongly correlated V $3d$ bands, illustrating that the effects of electron correlations are more pronounced in $CaVO_3$ than in $Sr_{0.5}Ca_{0.5}VO_3$, and that the surfaces of both materials are "more correlated" than their bulk [3]. Although valuable, comparisons between RXES and PES spectra are complicated by the quite different scattering processes and comparatively poorer resolution of RXES (owing, in part, to the broadening due to the lifetime of the core hole). In order to elicit quantitative information on the evolution of electron correlations from the surface to the bulk, depth-sensitive measurements using the same probe are clearly desired.

Hard x-ray photoemission spectroscopy (HAXPES) extends conventional PES measurements at ultraviolet and

*Present address: Department of Physics, IISER Bhopal, MP-462023, India.

soft x-ray energies into the hard x-ray regime ($\gtrsim$4 keV), yielding much greater depth sensitivity ($\gtrsim$5 nm compared with 0.5 nm at ultraviolet energies) [19]. However, at such hard energies, there are several additional considerations. Most importantly, the cross section for photoionization drops off at higher energies, particularly for shallow binding energies at the valence band [20], and practical instrument resolutions are poorer than at low energies. Additionally, the electron momentum distribution is focused into much tighter angles, meaning the coverage of the Brillouin zone of a typical HAXPES measurement is much broader, although recent technical advances have facilitated the momentum-resolved spectral function at hard x-ray energies [21].

We report here a HAXPES study of the electronic structure of $Sr_xCa_{1-x}VO_3$ using photon energies of 4.2 and 2.2 keV. The valence band of $Sr_xCa_{1-x}VO_3$ measured using 4.2 keV photons is quantitatively compared with *ab initio* theoretical calculations of the bulk, and we show that the spectra can be well described by band theory with some modest adjustments to the orbital-dependent photoionization cross sections. Additionally, we find that the evolution of the valence band electronic structure with x is dominated by different A-site hybridization. Second, the electronic structure of the correlated V 3d states is investigated as a function of distance into the sample from the surface. This was achieved by varying the photon energy of the HAXPES measurements, and by comparison with previous surface-sensitive ultraviolet photoemission spectroscopy (UPS) and unambiguously bulk-sensitive RXES measurements. Particular attention was paid to the *energetics* of the Hubbard subbands, which are one of the key properties in identifying the evolution of correlated behavior. We find that spectra recorded at 2.2 keV excitation energy still contain a large surface contribution of 30%–40%, despite photoelectrons at this energy often being considered bulk probes of correlated materials. However, we show that photoelectrons at 4.2 keV are found to essentially probe the bulk electronic structure. Significantly, we demonstrate that the correlated localized Hubbard bands evolve in both energy and spectral weight from the surface ("more correlated") of the material to the bulk ("less correlated"), in remarkable agreement with dynamical mean-field theory predictions.

II. METHODS

Large high-quality single crystals of $CaVO_3$ (CVO) and $Sr_{0.5}Ca_{0.5}VO_3$ (SCVO) were grown by the floating zone technique in a four-mirror optical furnace, employing growth rates of 7–10 mm/h in an atmosphere of 1 bar of Ar + 3% H_2 gas [3,22]. HAXPES measurements were performed at Beamline X24A of the National Synchrotron Light Source, Brookhaven National Laboratory, with a total instrument resolution (σ) of 180 meV at 2.2 keV and 220 meV at 4.2 keV. Photoelectrons with kinetic energies of 2.2 and 4.2 keV are estimated to have an IMFP, λ, of 3.6 and 6.1 nm, respectively, in $Sr_xCa_{1-x}VO_3$ within the TPP-2M model [23], compared with 0.5 nm at ultraviolet energies ($\sim$80 eV) [3,7]. Owing to the different densities of $CaVO_3$ and $SrVO_3$, the IMFP within this model is anticipated to be $\sim$8% smaller in $SrVO_3$ than in $CaVO_3$ (mean values, roughly corresponding to $Sr_{0.5}Ca_{0.5}VO_3$, are quoted above). Samples were cleaved *ex situ*, and immediately loaded into the ultrahigh vacuum chamber. The photoelectron energy was referenced to polycrystalline Ag in electrical contact with the sample.

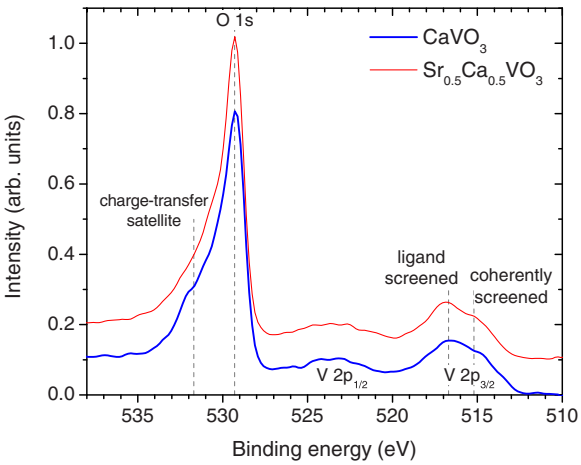

FIG. 1. (Color online) Core level HAXPES spectra at 4.2 keV of $CaVO_3$ and $Sr_{0.5}Ca_{0.5}VO_3$.

HAXPES measurements at 4.2 keV of the O 1s and V 2p core levels are shown in Fig. 1, and are in good agreement with previous reports at 1.8 keV [11]. The two compounds exhibit essentially identical core level spectra. The V $2p_{3/2}$ level exhibits two structures, originating from the ligand-screened and coherently screened final states of the photoemission process, and the $2p_{3/2}$ charge-transfer satellite is observed as a shoulder to the O 1s peak. These spectra are free of surface contaminant species and disorder effects, such as reports of V^{3+}/V^{5+} segregation at the surface of scraped samples [8,9]. We emphasize that the enhanced electron correlations at the surface that we discuss in Sec. IV are an *intrinsic* property of the surface, arising from the broken translational symmetry and reduced coordination [15], rather than an extrinsic surface problem (due to contaminant species and/or surface disorder).

Ab initio electronic structure calculations have been performed using the all-electron full-potential linearized augmented plane-wave (FLAPW) implemented by the ELK code [24], within the local density approximation (LDA) to the exchange-correlation functional. Experimental lattice parameters of 3.84 Å were used for cubic $SrVO_3$ [22] and $a = 5.32$ Å, $b = 5.34$ Å, and $c = 7.55$ Å were used for orthorhombic $CaVO_3$ [25]. Convergence was achieved over a $13 \times 13 \times 13$ mesh in the full Brillouin zone.

III. VALENCE BAND ELECTRONIC STRUCTURE

HAXPES measurements at 4.2 keV of the O 2p and V 3d valence band are shown for CVO and SCVO in Fig. 2(a). The O 2p states are characterized by a strong peak at -7 eV, with a prominent shoulder at -4 eV, above which the V 3d states are weakly visible as a double-peaked structure (and to which we return in more detail below). These spectra are in approximate agreement with previous PES measurements at low [12] and high [11] photon energies. For comparison, the total (broadened) density of states (DOS) from the FLAPW calculation, neglecting the energy-dependent photoionization cross section, is shown for the pure compounds at the bottom

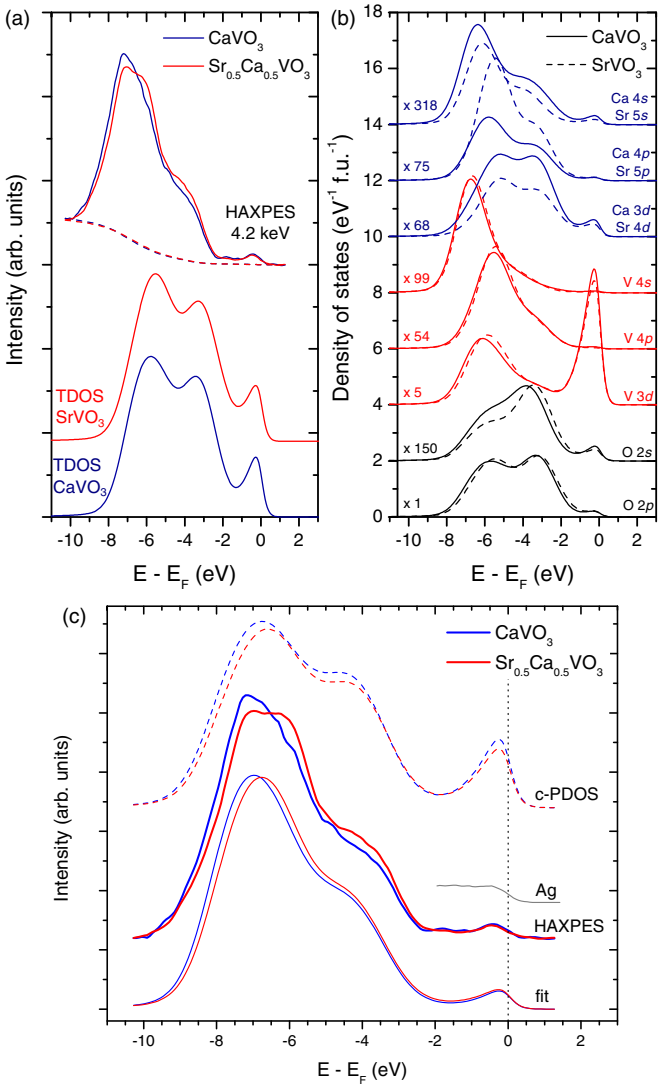

FIG. 2. (Color online) (a) HAXPES measurements at 4.2 keV of $CaVO_3$ and $Sr_{0.5}Ca_{0.5}VO_3$, illustrating the Shirley-type background contribution (dashed line). The broadened total DOS (TDOS) is shown at the bottom of the figure for $CaVO_3$ and $SrVO_3$. (b) Broadened partial densities of states of $CaVO_3$ and $SrVO_3$, showing the contribution from each orbital component, and their respective weights. Each curve has been offset vertically by 2 eV^{-1} $f.u.^{-1}$ for clarity. (c) HAXPES measurements after subtraction of the Shirley-type background, compared with the results of fitting the PDOS to the data (fit). Also shown is the theoretical cross-section corrected PDOS (c-PDOS).

of Fig. 2(a). In Fig. 2(b), the broadened occupied partial densities of states (PDOS) of $CaVO_3$ and $SrVO_3$ are shown, scaled (by a factor shown in the figure) to have approximately the same area. Whereas the total DOS are dominated by O $2p$ and V $3d$ character, the orbital-dependent photoionization cross section at $\approx$4 keV favors photoemission from the more localized s and p states. For example, the strength of the peak at -7 eV cannot be explained without a dramatic enhancement in the V sp and Ca/Sr s states, compared with the O $2p$ PDOS. Indeed, this is reflected in theoretical tabulations of these cross sections, which predict the Ca $4s$, Sr $5s$, and V $4s$ cross sections are between 13 and 21 times larger than the O $2p$ cross section at 4 keV [20].

In order to more accurately assess the origin of the differences in the HAXPES spectra between CVO and SCVO, we turn to a more quantitative analysis, in which the relative photoionization cross sections for each orbital are fitted to the experimental data, yielding approximate *empirical* relative cross sections. The data are first corrected for inelastic scattering processes, leading to the Shirley-type background shown by the dashed line in Fig. 2(a). The theoretical spectrum is then computed as a cross-section weighted sum of the orbital PDOS components shown in Fig. 2(b), neglecting the interstitial DOS (which, being delocalized away from the ion centers, are unlikely to contribute significantly at hard x-ray energies), and compared to the experimental spectrum. For SCVO, we take the rather crude approximation of 50% $CaVO_3$ PDOS and 50% $SrVO_3$ PDOS, although in practice this has only a very weak influence on the results; for example, comparing pure $SrVO_3$ with the SCVO data yields almost identical results.

The agreement between experiment and theory is optimized for both SCVO and CVO simultaneously using a single set of parameters. Additionally, the O $2p$ manifold is allowed to be rigidly shifted in energy during the fit, accounting for the inadequate description by the LDA of the V $3d$ bands. In the LDA FLAPW calculations, the LHB feature (the deeper of the two V $3d$ peaks) is absent, and so this rigid shift physically represents the experimental separation between the O $2p$ and *coherent* V $3d$ manifolds. Finally, the experimental broadening of the DOS is fitted through the convolution of the theoretical DOS with a Voigt function, $V(\sigma,\gamma) = G(\sigma) * L(\gamma)$, where $G(\sigma)$ is a Gaussian of width σ and $L(\gamma)$ is a Lorentzian of width γ. The results of the fit yield $\sigma = 0.67$ eV and $\gamma = 0.13$ eV, accounting for the total broadening due to both intrinsic and experimental resolution effects. All theoretical spectra in Fig. 2 have been convoluted with this function, and multiplied by a Fermi function of $k_B T_{\text{eff}} = 0.145$ eV [from a separate fit to the Fermi edge of polycrystalline Ag at 4.2 keV shown in Fig. 2(c)]. Although the solution from this fitting procedure is found to be relatively robust and stable, the extent to which the fitted parameters represent real photoionization cross sections must be considered with caution. For example, inaccuracies in the background subtraction and energy efficiency of the measurement may contribute nontrivially to the fit. Second, inadequacies of the LDA, which may under- or overestimate hybridization between orbital characters, may be strongly exaggerated, and the LHB feature is completely absent from the theoretical curve. Nevertheless, as we discuss below, the results do reflect physical expectations, and are interpreted as providing a reasonable indication of the trends of the orbital cross sections.

In Fig. 2(c), the results of the fit are shown alongside the background-corrected HAXPES spectra. A shift in the O $2p$ manifold downwards in energy by 0.9 eV is required to align the energies of the peaks in the theoretical and experimental spectra (the same shift is applied to both CVO and SCVO spectra). The fitted spectrum satisfyingly reproduces the experimental data, exhibiting the strong peak at -7 eV and its shoulder at -4 eV, as well as the rather weak relative intensity of the coherent V $3d$ states. Moreover, the weak upwards shift in energy of the lower peak at -7 eV of SCVO is

TABLE I. Orbital-dependent photoionization cross sections (CS) relative to the O $2p$ states according to the theoretical tabulations of Ref. [20] at 4 keV and from the results of fitting HAXPES spectra at 4.2 keV of CVO and SCVO to the FLAPW PDOS. The theoretical cross sections marked by an asterisk (*) correspond to nominally empty states that are not tabulated in Ref. [20]. Instead, for the A and V p states we adopt the corresponding s cross section, and for the Ca $3d$ and Sr $4d$ states we use the Sc $3d$ and Y $4d$ cross sections, respectively.

	Relative CS			Relative CS	
Orbital	Theory [20]	Fitted	Orbital	Theory [20]	Fitted
Ca $4s$	13.1	565.2	V $4s$	20.7	76.7
Ca $4p$	13.1*	57.3	V $4p$	20.7*	95.5
Ca $3d$	0.6*	0.2	V $3d$	1.7	0.4
Sr $5s$	16.6	737.3	O $2s$	38.5	0.1
Sr $5p$	16.6*	33.5	O $2p$	1.0	1.0
Sr $4d$	10.0*	131.9			

captured, along with the increase in the relative intensity of the shoulder. For comparison, the spectrum due to the theoretical cross sections [20] (labeled c-PDOS) is also shown (including the rigid shift of the O $2p$ manifold) in Fig. 2(c). Although this spectrum roughly reproduces the relative intensities (and energies) of the O $2p$ manifold, it strongly overestimates the contribution from the V $3d$ electrons. The fitted, empirical relative cross sections from the fit are shown in Table I, and exhibit the expected sensitivity of the HAXPES experiment to the more localized s and p states. Surprisingly, the relative O character is strongly suppressed, including the O $2s$ states, in contrast to other studies at similar energies (which do not attempt to optimize agreement between experiment and theory) [26,27]. However, it is clear from Fig. 2(b) that the shape of the O $2s$ PDOS is incompatible with the data. Finally, we note that incorporating an asymmetric Doniach-Šunjić line shape [28], which has recently been used to explain the HAXPES spectrum of V_2O_3 [27], does not improve agreement between experiment and theory.

Overall, these results establish that the experimental HAXPES spectra of $CaVO_3$ and $Sr_{0.5}Ca_{0.5}VO_3$ can be described well by the theoretical PDOS, with some modest adjustments to the theoretical orbital cross sections. Second, they demonstrate that the differences between the experimental spectra, in both relative intensity and energy, are mostly a consequence of the different A-site hybridization. The importance of A-site hybridization in $3d^1$ perovskites has been pointed out in detail by Ref. [29]. Finally, the effects of the A-site hybridization are more pronounced in the experimental spectra than predicted by theory.

IV. NEAR-E_F CORRELATED ELECTRONIC STRUCTURE

We now address the near-E_F electronic structure, which is dominated by the V $3d$ band. High-statistics spectra of the V $3d$ manifolds of CVO and SCVO at 4.2 and 2.2 keV are shown in Fig. 3, referenced to the Fermi level of polycrystalline Ag foil in electrical contact with the samples. As illustrated by the relatively large density of states at E_F, CVO and

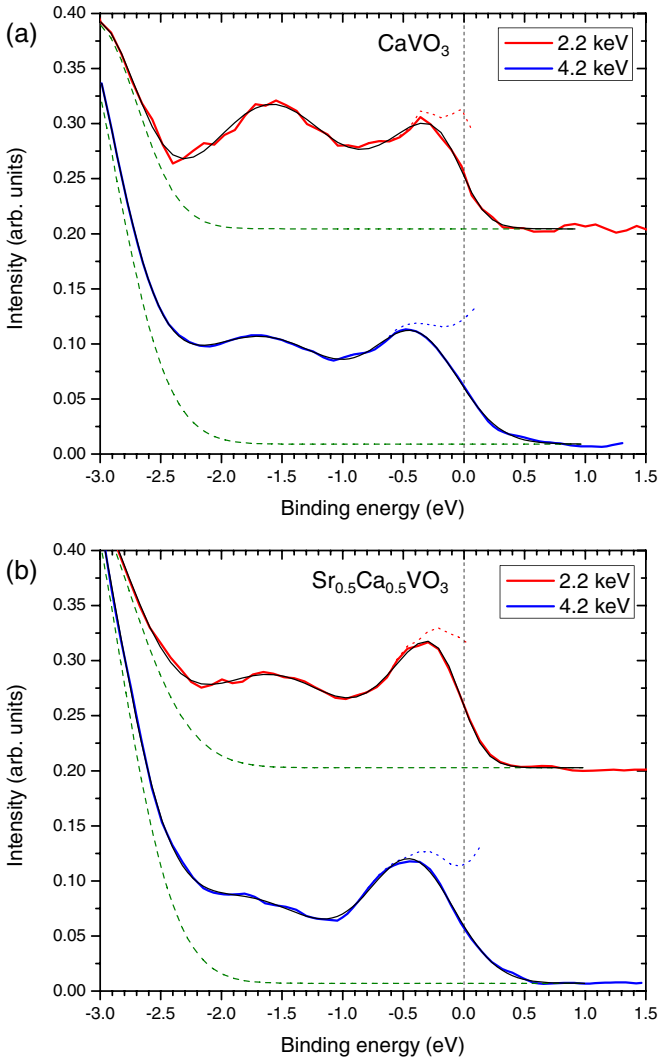

FIG. 3. (Color online) High-statistics HAXPES spectra of the V $3d$ states of (a) $CaVO_3$ and (b) $Sr_{0.5}Ca_{0.5}VO_3$ at 4.2 and 2.2 keV incident photon energies (vertically offset for clarity). The dashed (green) lines indicate the contributions from the tails of the O $2p$ band, and the black solid lines represent fits of the experimental spectra (see text). Finally, the dotted lines near E_F are the experimental spectra divided by the Fermi function (determined from Ag foil).

SCVO are both metallic in the HAXPES measurement, and consist of the O $2p$ tails below -2 eV, followed by the LHB near -1.5 eV and the QP at E_F. The dashed lines between -0.5 and 0 eV represent the same spectra after dividing by the "effective" Fermi function ($k_B T_{eff} = 120$ meV at 2.2 keV and 145 meV at 4.2 keV), reflecting approximately flat QP DOS up to E_F. The "effective" Fermi function is determined by fitting a Fermi function to the polycrystalline Ag reference spectra (displayed below in Fig. 5), and represents the total thermal and instrument resolution broadening. Similar observations of relatively flat DOS near E_F have been made using bulk-sensitive low-energy laser-PES at 7 eV [6]. In those measurements, performed with much higher resolution than is achievable at hard x-ray energies, a distinct drop-off of the QP DOS within 100 meV of E_F is observed in the extracted bulk component. Although we are unable to resolve such fine

details, our observation of flat DOS near E_F, coupled with the metallic nature of these spectra, demonstrate that recoil effects during the photoemission process at these energies are minor, and do not significantly shift the spectra, unlike other materials [30]. In addition to the broader resolution function, the integration over several Brillouin zones in the current HAXPES measurements also likely contributes to the flattening of the observed spectral weight near E_F.

In order to obtain quantitative information on the spectral weight and energetics of the LHB, the spectra in Fig. 3 have been fitted to a linear combination of three Gaussian components, with the results multiplied by the effective Fermi function. The results of this fit, which describe the data very well, are shown by the black solid lines in Fig. 3, and the dashed line indicates the component due to the tails of the O $2p$ states. The other two components represent photoelectrons from the LHB and QP, respectively.

A. Spectral weight

At both excitation energies shown in Fig. 3, the relative intensity of the QP is found to be smaller in CVO than it is in SCVO, which is consistent with the common notion that CVO is "more correlated." In CVO, the narrower bandwidth W of the V $3d$ states means the relative importance of electron correlations, often parametrized through U/W, is greater (the Coulomb energy U is not expected to evolve between $SrVO_3$ and $CaVO_3$ [14]).

In order to investigate how the spectral weight varies with HAXPES excitation energy, we show the fitted spectra normalized to the intensity of the LHB in Fig. 4(a), alongside the UPS results of Ref. [3]. To aid comparison, all spectra in Fig. 4(a) have been broadened to have the same instrument resolution function of $\sigma = 220$ meV (i.e., the resolution of the 4.2 keV HAXPES measurement). Figure 4(a) illustrates that the QP spectral weight is suppressed in the more surface-sensitive 2.2 keV HAXPES measurement. Since both the QP and LHB features derive from the same V $3d$ states, their photoionization cross section is the same, and therefore this evolution can be directly associated with the different depth sensitivities of the two measurements. The UPS spectra do not follow this trend; however, these spectra were recorded on oriented samples near the Γ point of the Brillouin zone, and therefore represent a quite different (and specific) subset of momentum space.

Similar suppression in the QP weight with increasing surface sensitivity has previously been reported at lower photon energies [4,8,9]. This observation suggests that there is an *intrinsic* surface component of the electronic structure that is significantly "more correlated" than the bulk in both materials. Moreover, it indicates that an excitation energy of 2.2 keV is not sufficient to represent the bulk electronic structure of these materials. Previous efforts to extract bulk information from $Sr_xCa_{1-x}VO_3$ have focused on PES at soft x-ray energies up to 900 [4], 275 [9], or 1486 eV [8] (although bulk-sensitive laser-PES has also been used [6], the LHB lies outside the experimental range). These have yielded conflicting pictures of the bulk electronic structure, for example, whether it is independent of x or not. Our measurements illustrate that hard x rays above ~4 keV are required to truly examine the bulk using photoemission.

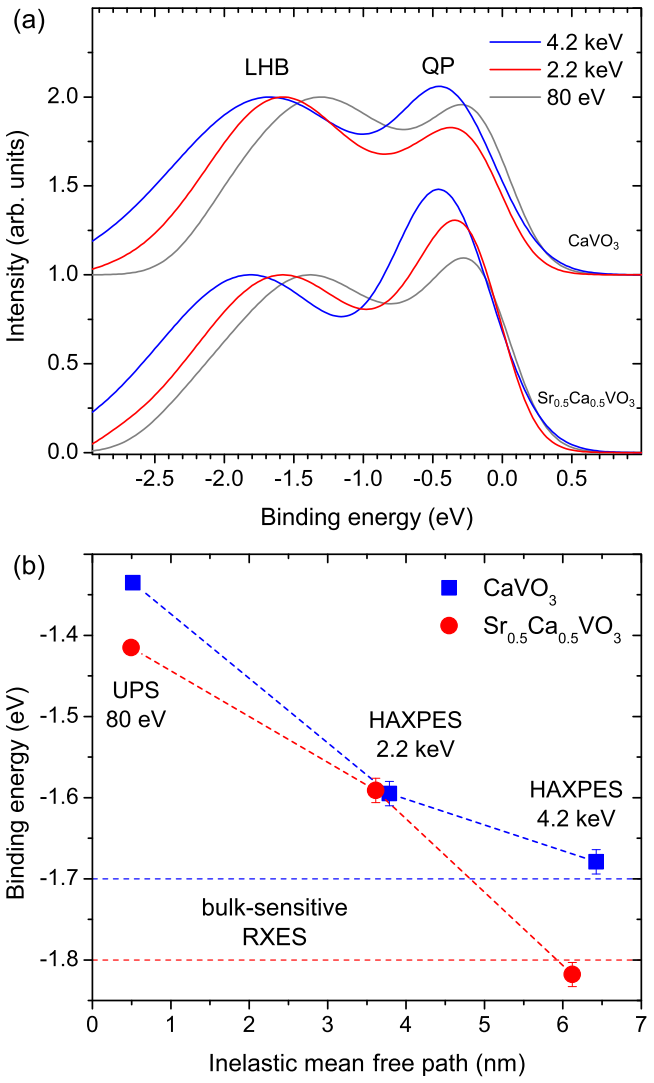

FIG. 4. (Color online) Results of fitting the HAXPES spectra to Gaussian components. (a) Fitted spectra (excluding the O $2p$ tails) shown alongside the UPS spectra of Ref. [3]. All spectra have been broadened to have the same effective instrument resolution function, corresponding to $\sigma = 220$ meV, and normalized to the intensity of the LHB. (b) Binding energy of the LHB for the two compounds, shown as a function of the estimated IMFP, λ. The horizontal dashed lines indicate the separation between the QP and LHB from bulk-sensitive RXES [3]. The error bars represent estimated statistical errors associated with the fitting.

B. Binding energy

Whereas changes in the spectral weight of the QP and LHB are useful indications of correlated electron behavior, extracting such quantitative information from experiments can be complicated by overlapping extrinsic surface species and the tails of the O $2p$ states, as well as the details of the Brillouin zone coverage. We now turn to the *energetics* of the LHB, which are experimentally much more robust, particularly since the LHB is not dispersive in momentum [12,16]. As can be seen in Figs. 3 and 4, the energy of the LHB in both compounds lies at deeper energies in the 4.2 keV spectrum than

at 2.2 keV, consistent with stronger electron correlations at the surface.

At 4.2 keV, the LHB is found at −1.68 and −1.82 eV for CVO and SCVO, respectively (Fig. 4), which compares very well with the separation between the QP and LHB observed in truly bulk-sensitive RXES measurements [3]. Qualitatively, these results are in agreement with dynamical mean-field theory (DMFT) calculations of $CaVO_3$ and $SrVO_3$ using the same Coulomb parameter U [14]. HAXPES at this energy can be considered representative of the bulk correlated electronic structure. At 2.2 keV the LHBs of both compounds are located at −1.59 eV, which is in rough agreement with the x-independent soft x-ray results [4]. We discuss these spectra in more detail below, including the similarity in the LHB energy of both compounds. At the surface, UPS suggests a markedly shallower energy for the LHB of −1.34 and −1.42 eV, respectively, which is ∼20% closer to E_F than in the bulk. The evolution in correlated electron behavior between the surface and the bulk has been investigated by Ishida *et al.* through LDA + DMFT calculations of the VO_2- and SrO-terminated surfaces of $SrVO_3$ [15]. At the VO_2-terminated surface, the overall effect on the energy of the LHB is only weak, partly due to the emptying of the in-plane d_{xy} surface orbital. On the other hand, in good agreement with our results, these calculations find that the LHB is located at −1.6 eV in the bulk and −1.2 eV at the SrO-terminated surface, and that the LHB has substantially greater spectral weight at the surface. This reduction in the binding energy of the correlated Hubbard bands, which is reproduced for both unrelaxed and relaxed SrO-terminated surfaces, arises intrinsically due to the reduced coordination of the V ions at the surface, and the subsequent narrowing of the bandwidth of the out-of-plane $d_{xz,yz}$ orbitals [15].

C. 2.2 keV HAXPES

Having established the variation in the energy and spectral weight of the LHB with depth, we now briefly discuss some of the implications of the spectra recorded at 2.2 keV. In particular, the energies of the LHBs of both compounds are significantly shallower than in the bulk, and are very similar for the two different compounds, despite their differences at both the surface and the bulk. If we consider that the 2.2 keV spectra contain distinct surface and bulk components, it is possible to adequately fit the data using LHB and QP energies representative of the surface (UPS) and bulk (4.2 keV HAXPES). Under this assumption, 29% and 45% of the 2.2 keV HAXPES signal of CVO and SCVO, respectively, is found to correspond to the surface signal. Indeed, this simple model reflects the larger surface sensitivity of identical photoemission measurements on $SrVO_3$ compared with $CaVO_3$, which is due to the higher density of $SrVO_3$ and therefore shorter IMFP.

However, the results at 2.2 keV do not agree well with simple calculations of the expected surface contribution. Based on the IMFP, λ, the surface contribution can be expressed as $1 - \exp(-s/\lambda)$, where s is the thickness of the surface layer. Assuming a surface layer of 7.5 Å [4], the surface contribution is 18% and 11% at 2.2 and 4.2 keV, respectively, with only a very minor difference (∼0.5%) between compounds. This is not only at odds with the results presented above, but it is also impossible to find a reasonable value of the surface thickness at which 2.2 keV photoelectrons are significantly (e.g., more than two times) more sensitive to than 4.2 keV photoelectrons. It therefore appears that either the distribution of detected photoelectrons from the sample is not simply an exponential decay, or that the notion of a definite, discrete correlated surface layer is incorrect. The second possibility seems less likely based on LDA and DMFT calculations, in which changes to the electronic (and, indeed, crystal) structure due to the surface were found to decay very rapidly from the surface [15]. In either case, it calls into question one of the common methods of extracting bulk contributions from PES, at least applied to studying correlated electron behavior [4,6,8,9], in which a spectrum at a single photon energy is assumed to be composed of discrete surface and bulk contributions weighted by the exponential decay due to the IMFP. In our data, it is not possible to reproduce either surface or bulk spectra by such a method.

D. Summary

In Fig. 5, the O 2p tails have been subtracted from the spectra, and the results have been compiled with the UPS and RXES measurements of Ref. [3], which were recorded on the same samples as used in this study. In this figure, the RXES spectra, which represent transitions from the valence band into the V $2p_{3/2}$ core level, have been shifted in energy by 515.2 eV, corresponding to the coherently screened V $2p_{3/2}$ HAXPES core level in Fig. 1. The light gray lines show spectra of polycrystalline Ag at 2.2 and 4.2 keV for comparison,

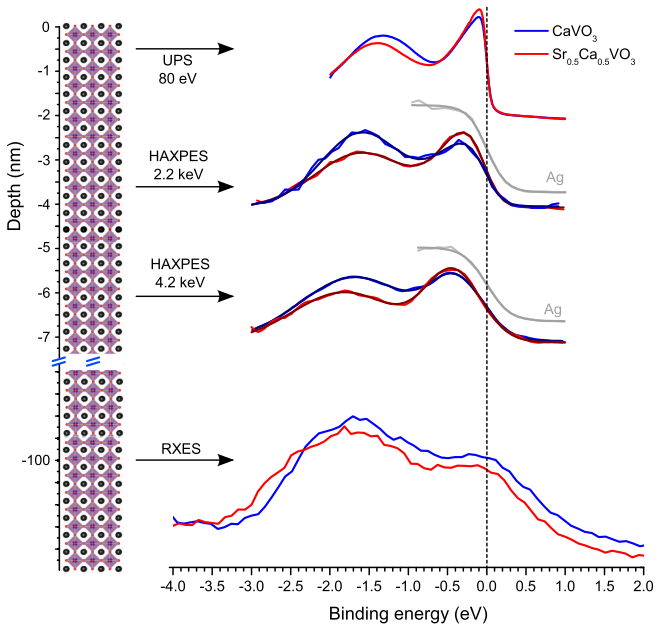

FIG. 5. (Color online) Comparison between various probes of different depth sensitivities of the correlated electronic structure of $CaVO_3$ and $Sr_{0.5}Ca_{0.5}VO_3$. The approximate depth sensitivity of each technique is illustrated on the left, with reference to the SrO-terminated surface of cubic $SrVO_3$(100). The HAXPES spectra are those shown in Fig. 3 after subtraction of the O 2p tails. Corresponding Ag reference spectra recorded at the same energies are also shown. The UPS and RXES results are from Ref. [3].

underlying the metallicity of the $CaVO_3$ and $Sr_{0.5}Ca_{0.5}VO_3$ measurements. In Fig. 5, the evolution in energy of the LHB from the surface (UPS) to the bulk (4.2 keV HAXPES) can be clearly seen, as well as the agreement in energy of the LHB in the bulk HAXPES and the RXES spectra.

In summary, our results illustrate the evolution in correlated electron behavior from the surface of $CaVO_3$ and $Sr_{0.5}Ca_{0.5}VO_3$ to the bulk. Spectra at 4.2 keV agree very well with truly bulk-sensitive RXES measurements, and are considered representative of the bulk correlated electronic structure. On the other hand, spectra at 2.2 keV are in good agreement with those at soft x-ray energies [4], but are not bulklike and still contain a surface signal of 30%–40%. We also find that reliable surface and bulk components cannot be extracted from intermediate spectra, indicating that either the surface layer is not a discrete overlayer to the bulk, or that detected photoelectrons do not originate from an exponential distribution within the sample.

Signatures of evolving electron correlations are observed in both the spectral weight of the QP and LHB and in the binding energy of the LHB. At both the surface and in the bulk, $CaVO_3$ is found to be "more correlated" than $Sr_{0.5}Ca_{0.5}VO_3$: The correlated LHB of $CaVO_3$ exhibits greater spectral weight and is located closer to E_F than in $Sr_{0.5}Ca_{0.5}VO_3$, in good agreement with predictions from DMFT of $CaVO_3$ and $SrVO_3$ [14]. At the surface, the spectral weight of the LHB of both compounds is enhanced, and is ∼20% closer to E_F than in the bulk, indicating significantly stronger electron correlations at the surface. This result is in very good agreement with DMFT calculations of the SrO-terminated $SrVO_3$(001) surface, which indicate a 25%–40% decrease in binding energy of the LHB at the surface [15].

V. CONCLUSION

We have presented a detailed HAXPES study of the electronic structure of $Sr_xCa_{1-x}VO_3$. Measurements of the valence band have been quantitatively compared with *ab initio* calculations within the LDA, and are found to be in good agreement after some modest empirical adjustments to the orbital-dependent photoionization cross sections, with the *A*-site hybridization in the O $2p$ manifold mostly responsible for the differences between compounds. Second, our results on the correlated V $3d$ bands support $CaVO_3$ as being a "more correlated" metal than $SrVO_3$, and illustrate the significant enhancement in electron correlations at the surface compared with the bulk. The results are found to be in good agreement with DMFT predictions of the evolution in the spectral function with x and between the surface and the bulk. Finally, we resolve the long-standing controversy of efforts to extract bulk information from PES by showing that photoelectrons of $\gtrsim$4 keV are required to obtain truly bulk-representative spectra.

ACKNOWLEDGMENTS

The Boston University program is supported in part by the Department of Energy under Grant No. DE-FG02-98ER45680. This work is also supported in part by the Boston University/University of Warwick collaboration fund. The National Synchrotron Light Source, Brookhaven, is supported by the US Department of Energy under Contract No. DE-AC02-98CH10886. Additional support was provided by the National Institute of Standards and Technology. G.B. gratefully acknowledges financial support from EPSRC Grant No. EP/I007210/1.

[1] J. Chakhalian, A. J. Millis, and J. Rondinelli, Nat. Mater. **11**, 92 (2012); P. Zubko, S. Gariglio, M. Gabay, P. Ghosez, and J.-M. Triscone, Annu. Rev. Condens. Matter Phys. **2**, 141 (2011).

[2] G. Kotliar, S. Y. Savrasov, K. Haule, V. S. Oudovenko, O. Parcollet, and C. A. Marianetti, Rev. Mod. Phys. **78**, 865 (2006).

[3] J. Laverock, B. Chen, K. E. Smith, R. P. Singh, G. Balakrishnan, M. Gu, J. W. Lu, S. A. Wolf, R. M. Qiao, W. Yang, and J. Adell, Phys. Rev. Lett. **111**, 047402 (2013).

[4] A. Sekiyama, H. Fujiwara, S. Imada, S. Suga, H. Eisaki, S. I. Uchida, K. Takegahara, H. Harima, Y. Saitoh, I. A. Nekrasov, G. Keller, D. E. Kondakov, A. V. Kozhevnikov, Th. Pruschke, K. Held, D. Vollhardt, and V. I. Anisimov, Phys. Rev. Lett. **93**, 156402 (2004).

[5] T. Yoshida, K. Tanaka, H. Yagi, A. Ino, H. Eisaki, A. Fujimori, and Z.-X. Shen, Phys. Rev. Lett. **95**, 146404 (2005); S. Aizaki, T. Yoshida, K. Yoshimatsu, M. Takizawa, M. Minohara, S. Ideta, A. Fujimori, K. Gupta, P. Mahadevan, K. Horiba, H. Kumigashira, and M. Oshima, *ibid.* **109**, 056401 (2012).

[6] R. Eguchi, T. Kiss, S. Tsuda, T. Shimojima, T. Mizokami, T. Yokoya, A. Chainani, S. Shin, I. H. Inoue, T. Togashi, S. Watanabe, C. Q. Zhang, C. T. Chen, M. Arita, K. Shimada, H. Namatame, and M. Taniguchi, Phys. Rev. Lett. **96**, 076402 (2006).

[7] T. Yoshida, M. Hashimoto, T. Takizawa, A. Fujimori, M. Kubota, K. Ono, and H. Eisaki, Phys. Rev. B **82**, 085119 (2010).

[8] K. Maiti, D. D. Sarma, M. J. Rozenberg, I. H. Inoue, H. Makino, O. Goto, M. Pedio, and R. Cimino, Europhys. Lett. **55**, 246 (2001).

[9] K. Maiti, U. Manju, S. Ray, P. Mahadevan, I. H. Inoue, C. Carbone, and D. D. Sarma, Phys. Rev. B **73**, 052508 (2006).

[10] H. F. Pen, M. Abbate, A. Fujimori, Y. Tokura, H. Eisaki, S. Uchida, and G. A. Sawatzky, Phys. Rev. B **59**, 7422 (1999); R. J. O. Mossanek, M. Abbate, T. Yoshida, A. Fujimori, Y. Yoshida, N. Shirakawa, H. Eisaki, S. Kohno, P. T. Fonseca, and F. C. Vicentin, J. Phys.: Condens. Matter **22**, 095601 (2010).

[11] R. J. O. Mossanek, M. Abbate, T. Yoshida, A. Fujimori, Y. Yoshida, N. Shirakawa, H. Eisaki, S. Kohno, and F. C. Vicentin, Phys. Rev. B **78**, 075103 (2008).

[12] M. Takizawa, M. Minohara, H. Kumigashira, D. Toyota, M. Oshima, H. Wadati, T. Yoshida, A. Fujimori, M. Lippmaa, M. Kawasaki, H. Koinuma, G. Sordi, and M. Rozenberg, Phys. Rev. B **80**, 235104 (2009).

[13] A. Liebsch, Phys. Rev. Lett. **90**, 096401 (2003).

[14] I. A. Nekrasov, G. Keller, D. E. Kondakov, A. V. Kozhevnikov, Th. Pruschke, K. Held, D. Vollhardt, and V. I. Anisimov, Phys. Rev. B **72**, 155106 (2005).

[15] H. Ishida, D. Wortmann, and A. Liebsch, Phys. Rev. B **73**, 245421 (2006).
[16] I. A. Nekrasov, K. Held, G. Keller, D. E. Kondakov, Th. Pruschke, M. Kollar, O. K. Andersen, V. I. Anisimov, and D. Vollhardt, Phys. Rev. B **73**, 155112 (2006).
[17] K. Byczuk, M. Kollar, K. Held, Y.-F. Yang, I. A. Nekrasov, Th. Pruschke, and D. Vollhardt, Nat. Phys. **3**, 168 (2007); M. Gatti and M. Guzzo, Phys. Rev. B **87**, 155147 (2013); R. Sakuma, Ph. Werner, and F. Aryasetiawan, *ibid.* **88**, 235110 (2013).
[18] K. Yoshimatsu, T. Okabe, H. Kumigashira, S. Okamoto, S. Aizaki, A. Fujimori, and M. Oshima, Phys. Rev. Lett. **104**, 147601 (2010); M. Gu, J. Laverock, B. Chen, K. E. Smith, S. A. Wolf, and J. Lu, J. Appl. Phys. **113**, 113704 (2013).
[19] C. S. Fadley, Nucl. Instrum. Methods Phys. Res., Sect. A **547**, 24 (2005).
[20] M. B. Trzhaskovskaya, V. I. Nefedov, and V. G. Yarzhemsky, At. Data Nucl. Data Tables **77**, 97 (2001).
[21] A. X. Gray, C. Papp, S. Ueda, B. Balke, Y. Yamashita, L. Plucinski, J. Minár, J. Braun, E. R. Ylvisaker, C. M. Schneider, W. E. Pickett, H. Ebert, K. Kobayashi, and C. S. Fadley, Nat. Mater. **10**, 759 (2011).
[22] I. H. Inoue, O. Goto, H. Makino, N. E. Hussey, and M. Ishikawa, Phys. Rev. B **58**, 4372 (1998).
[23] S. Tanuma, C. J. Powell, and D. R. Penn, Surf. Interface Anal. **21**, 165 (1994).
[24] J. K. Dewhurst, S. Sharma, L. Nordström, F. Cricchio, F. Bultmark, and E. K. U. Gross, http://elk.sourceforge.net (2012).
[25] H. Falcón, J. A. Alonso, M. T. Casais, M. J. Martínez-Lope, and J. Sánchez-Benítez, J. Solid State Chem. **177**, 3099 (2004).
[26] J. C. Woicik, E. J. Nelson, L. Kronik, M. Jain, J. R. Chelikowsky, D. Heskett, L. E. Berman, and G. S. Herman, Phys. Rev. Lett. **89**, 077401 (2002).
[27] J. C. Woicik, M. Yekutiel, E. J. Nelson, N. Jacobson, P. Pfalzer, M. Klemm, S. Horn, and L. Kronik, Phys. Rev. B **76**, 165101 (2007).
[28] S. Doniach and M. Šunjić, J. Phys. C **3**, 285 (1970).
[29] E. Pavarini, A. Yamasaki, J. Nuss, and O. K. Andersen, New J. Phys. **7**, 188 (2005).
[30] S. Suga, A. Sekiyama, H. Fujiwara, Y. Nakatsu, T. Miyamachi, S. Imada, P. Baltzer, S. Niitaka, H. Takagi, K. Yoshimura, M. Yabashi, K. Tamasaku, A. Higashiya, and T. Ishikawa, New J. Phys. **11**, 073025 (2009).